



Impact of Annealing Temperature on Physical Properties of Manganese Sulfide Thin Film

Tuba ÇAYIR TAŞDEMİRÇİ^{1,*} 

¹ Department of Biomedical Engineering, Erzincan Binali Yıldırım University, Erzincan, Türkiye, **ORCID:** 0000-0001-9519-8483

Article Info

Research paper

Received : October 7, 2024

Accepted : April 22, 2025

Keywords

MnS
Thin Film
Annealing Temperature
SILAR

Abstract

MnS thin films were grown on glass substrates at room temperature using the SILAR method, which is simple, easy to apply, and cheap. The grown thin films were annealed at 150, 200, 250, and 300°C for 30 minutes, respectively. The structural and optical properties of the obtained thin films were examined. XRD and SEM analyses were performed for structural properties, and UV-Vis analyses were performed for optical properties. Based on the results, it can be concluded that the annealing temperature has a positive impact on the structural and optical properties of MnS thin films.

1. Introduction

In recent years, chalcogenide films have been widely used in solar energy applications as sensors, optical mass memories, photoconductors, and buffer materials. Manganese Sulfide, one of the chalcogenide films, is a p-type semiconductor with a wide band gap of approximately 3.7eV [1]. MnS is a material used in magnetic properties due to its wide band gap, short wavelength and optoelectronic fields. MnS exists in three different phases in nature. α -MnS is the green stable form (albandite) with a rock-salt structure, whereas β -MnS and γ -MnS are metastable modifications with sphalerite (ZB) and wurtzite (W) structures, respectively [2]. MnS metastable states have many chemical properties. Many methods are used to grow thin metal chalcogenide films onto glass, metal, and other substrates. These methods include hydrothermal [3], RF sputtering [4], chemical bath deposition (CBD) [5-9], SILAR [10-15], thermal evaporation [16,17], aerosol-assisted chemical vapour deposition (AACVD) [18], etc. Methods such as these can be given as examples. Among

these methods, the SILAR method is very easy and controllable.

Yıldırım et. al. synthesized MnS thin films on glass substrates using the SILAR method. They studied the effect of film thickness on the structural, morphological, optical and electrical properties of the films, and found that the β -MnS phase had a polycrystalline structure, the band gap value decreased from 3.39 eV to 2.92 eV, and the film thickness increased from 180nm to 350nm. Chaki et. al. MnS thin film was deposited on a glass substrate using the chemical bathing technique. XRD results showed that it has a hexagonal structure in the gamma phase. UV-Vis results showed that the direct and indirect optical band gap values of MnS thin films were 3.67 eV to 2.67 eV. Yang et. al. deposited compact MnCoS thin films (SILAR) on nickel foam (NF) substrate. Two surfactants (SDS and CTAB) were used to improve the wettability of NF. Scanning electron microscopy (SEM), transmission electron microscopy (TEM), X-ray diffraction (XRD), and X-ray photoelectron spectroscopy (XPS) methods were used to characterize the MnCoS thin films. Through the

* Corresponding Author: tcayir@erzincan.edu.tr



electrostatic interaction between the charged ionic groups of the surfactant and the MnCoS nanoparticles, the charge of the particles deposited on the nickel foam surface increased significantly and formed a dense film, and finally, it was found to improve the specific capacity of the active material significantly. [19-21] This article reports on the production and characterization of MnS thin films with SILAR. The effect of annealing temperature on the optical and structural properties of MnS thin films was examined. The annealing temperature is a parameter that enables significant changes in the structure of the thin film. This study investigates the changes in the structural and optical properties of MnS thin films due to annealing temperature. These temperatures have been selected to observe phase transformations and crystallinity improvements in MnS without causing unwanted decomposition or oxidation. Lower temperatures (below 150°C) might not provide sufficient energy for structural reorganization or grain growth. Higher temperatures (above 300°C) might lead to excessive grain growth, oxidation, or degradation of the thin film. The glass substrate has a thermal limit, and exceeding certain temperatures could cause deformation, warping, or stress-induced defects. Choosing temperatures up to 300°C ensures film improvement while maintaining the integrity of the substrate. When MnS semiconductor thin films are grown at room temperature, they mostly occur in the gamma phase. When exposed to heat, they transform into the beta phase, and when exposed to higher temperatures, they transform into the alpha phase [4, 22]. The results obtained from many studies support this situation. MnS thin films have been grown using many methods in literature. However, the number of studies using the SILAR method is quite low. In addition, the studies have obtained results that the MnS thin film is in gamma or beta phase at room temperature. The aspect that distinguishes this study from other studies is that the beta and alpha phases are obtained.

2. Materials and Methods

To grow MnS thin films, glass substrate materials are sterilized. The glass substrate is first cleaned with deionized water, then with sulfuric acid for 10 minutes, then with

acetone. Finally, it is made ready by cleaning with deionized water. When the substrate material is ready, the MnS solution is prepared. For the MnS solution, 0.1M MnCl₂ is prepared as the cationic solution and 0.05M Na₂S solution is prepared as the anionic solution. 100 mL of deionized water is used to prepare the solutions. To regulate the pH level of the solution, the ammonia (NH₃) compound is added to the MnCl₂ solution at a ratio of 1:10. Thus, the solutions are ready.

SILAR method growth stages of MnS thin film;

In Stage 1; The glass substrate is dipped into a MnCl₂ solution for 30 seconds, allowing Mn and loosely attached Cl ions to bind to the surface of the glass.

In Stage 2; The glass substrate is placed in deionized water for 60 seconds, during which the weakly bound Cl ions on the surface are removed.

In Stage 3; The glass substrate is placed in the Na₂S solution for 30 seconds, and at this stage, Na and S ions adhere to the surface.

In Stage 4; The glass substrate is immersed in deionized water for 60 seconds, during which weakly bound Na ions are removed from the surface, completing a SILAR cycle. This process is repeated until a uniform coating is achieved on the surface. A schematic representation of the SILAR method is given in Figure 1. This study performed 160 rounds of SILAR cycles to grow MnS thin films. Table 1 gives the parameters used for the MnS thin film.

Table 1. Optimized deposition parameters for MnS thin film.

Deposition Parameters	Cationic Precursor	Anionic Precursor
Precursor	MnCl ₂	Na ₂ S
Concentration	0.1 M	0.05M
Immersion Time	30s	30s
Rising Time	60s	60s
Volume of Precursor	100mL	100mL

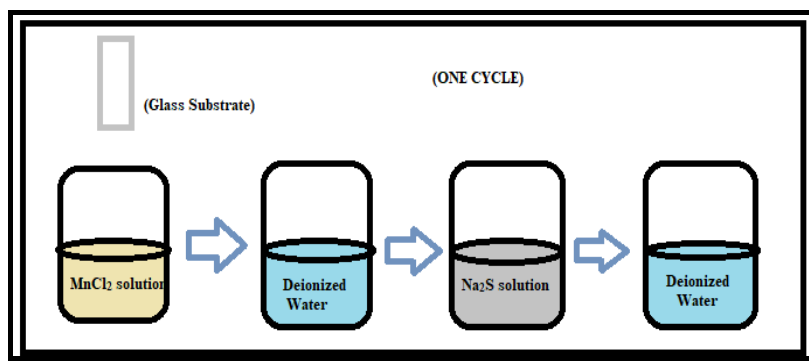


Figure 1. A diagrammatic illustration of the SILAR method

3. Results and Discussion

Figure 2 shows the XRD patterns of MnS thin films. XRD measurements were made in the range of the 2θ angle 20-70. XRD findings demonstrated that MnS thin films have a polycrystalline and cubic structure and have both α-MnS and β-MnS phases.

This conclusion was reached by looking at JPCDS:03-065-0891 and JPCDS:40-1288. In the α-MnS phase, the XRD peaks were in the (111), (200), (311) and (222) orientations, while in the β-MnS phase, the XRD peaks were in the (102) and (220) orientations. It is seen that as the annealing temperature increases; the peak intensities also increase.

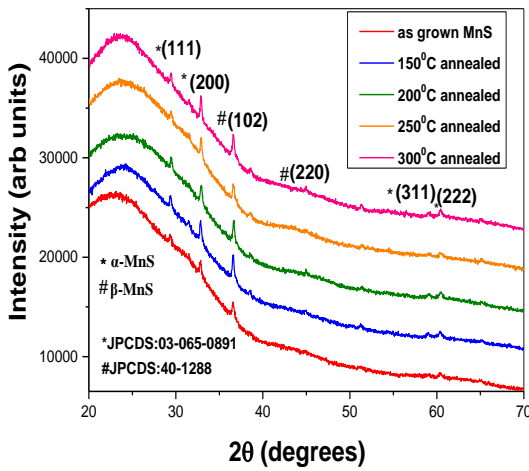


Figure 2. The XRD patterns of MnS thin films unannealed, 150°C annealed, 200°C annealed, 250°C annealed, 300°C annealed.

Debye Scherrer's formula for calculating grain size [23]

$$D = \frac{0.9\lambda}{\beta \cos\theta} \quad (1)$$

D= Grain size, λ=Wavelength, β= Half peak width (FWHM), θ= Bragg's angle.

The dislocation density for the (200) plane is evaluated using the following relation [24]

$$\delta = \frac{1}{D^2} \quad (2)$$

According to the calculations, the grain size value was 11.66 nm for the unannealed MnS thin film, while it was obtained as 13.36 nm at 150°C, 18.41 nm at 200°C, 30.68 nm at 250°C and 43.6 nm at 300°C, respectively, with the effect of annealing temperature. As the annealing temperature increased, the grain size of the MnS thin films increased, while the half peak width (FWHM) decreased from 0.71 to 0.19. Dislocation density values were also calculated in line with the obtained D value, and as the film thickness increased, the dislocation density value decreased

from $73 \times 10^{-4} \text{cm}^{-2}$ to $5 \times 10^{-4} \text{cm}^{-2}$. As annealing temperature increases, grain size typically increases due to grain growth and recrystallization. This leads to reduced grain boundaries, which often improves the material's overall properties. Larger grains indicate fewer defects and better crystallinity. Dislocation density is a measure of the number of dislocations (defects in the crystal lattice) per unit area. Higher annealing temperatures generally reduce dislocation density because of defect annihilation and reordering of the crystal lattice during thermal treatment. Lower dislocation density corresponds to improved crystal quality and fewer internal stresses. FWHM is the width of an XRD peak at half its maximum intensity and is inversely related to the crystal size. A narrower FWHM indicates better crystallinity, with larger and more uniform crystallites. As annealing temperature increases, FWHM typically decreases, confirming improved structural ordering. Smaller grain size, higher dislocation density, and broader FWHM suggest more defects, poorer crystallinity, and smaller crystallites. Larger grain size, lower dislocation density, and narrower FWHM suggest better crystallinity, reduced defects, and larger, well-formed crystallites. The improvements in D, δ, and FWHM at the (200) plane with increasing annealing temperature indicate that this orientation becomes more dominant and better crystallized. This enhancement suggests that the material becomes more ordered and suitable for applications where high-quality MnS thin films are required. Table 2 presents the dislocation density (δ), grain size (D), and full width at half maximum (FWHM) values for the most prominent (200) peak of MnS thin films.

Table 2. Dislocation density (δ), Grain size (D), and full width at half maximum (FWHM) values for the most prominent (200) peak of MnS thin films.

MnS	Unannealed	150°C	200°C	250°C	300°C
D(nm)	11.66	13.36	18.41	30.68	43.6
FWHM	0.71	0.62	0.45	0.27	0.19
δ*10 ⁻⁴ (nm ⁻²)	73	56	29	10	5

Figure 3 shows the SEM images of unannealed MnS thin films annealed at 150°C, 200°C, 250°C, and 300°C. In Figure 3(a), it is seen that there is a coating in the form of broken spheres on the surface in the SEM image of the unannealed MnS thin film. In Figure 2(b, c, d, e), it is seen that the grain sizes of these spheres increase and the surface morphology becomes better with the increase of the annealing temperature. Similar SEM images were obtained by Biswas et al., where MnS thin films were deposited by solvothermal synthesis, and Zhao et al., where MnS films were grown by the hydrothermal method [3, 25].

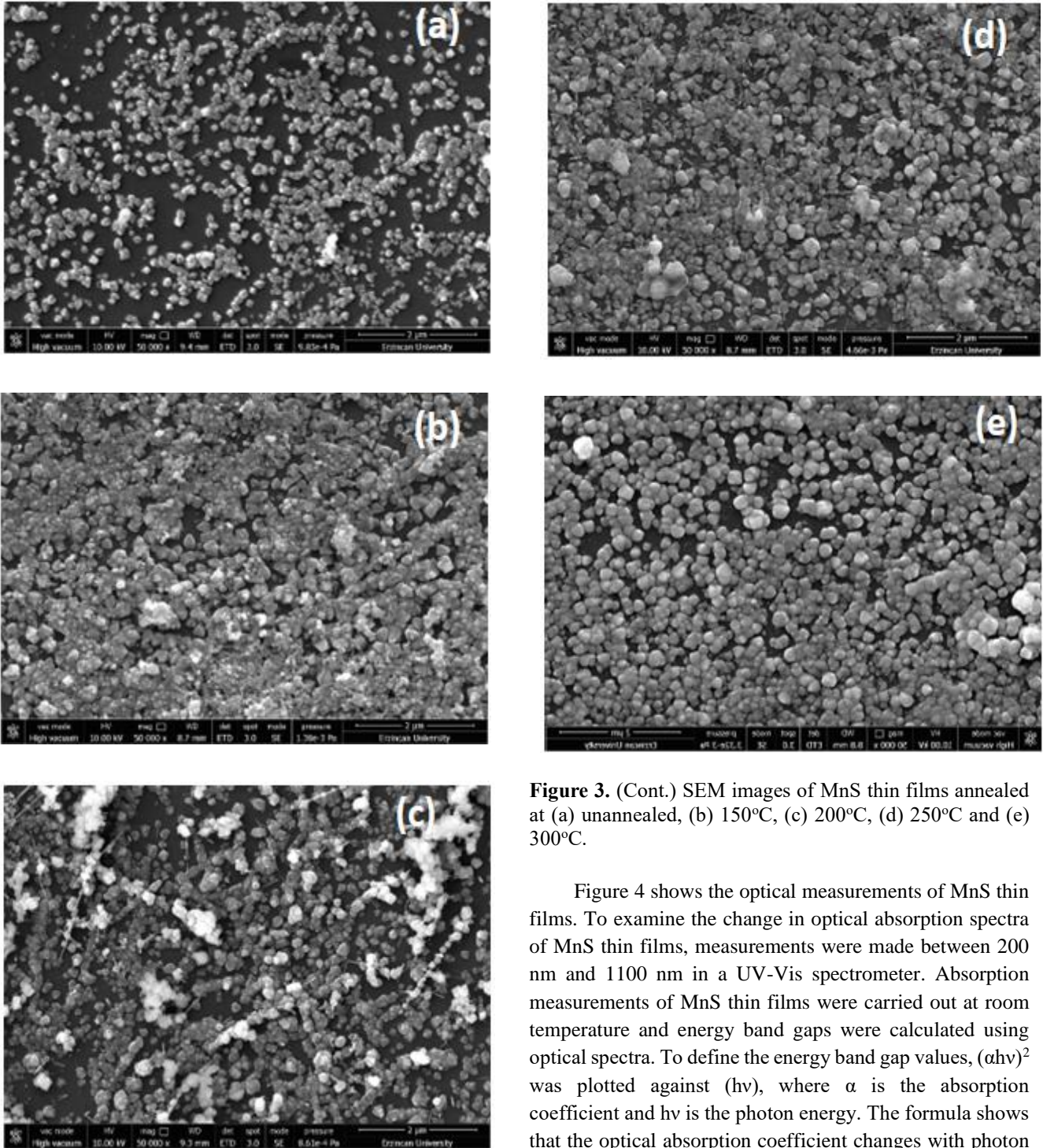


Figure 3. SEM images of MnS thin films annealed at (a) unannealed, (b) 150°C, (c) 200°C, (d) 250°C and (e) 300°C.

Figure 3. (Cont.) SEM images of MnS thin films annealed at (a) unannealed, (b) 150°C, (c) 200°C, (d) 250°C and (e) 300°C.

Figure 4 shows the optical measurements of MnS thin films. To examine the change in optical absorption spectra of MnS thin films, measurements were made between 200 nm and 1100 nm in a UV-Vis spectrometer. Absorption measurements of MnS thin films were carried out at room temperature and energy band gaps were calculated using optical spectra. To define the energy band gap values, $(\alpha h\nu)^2$ was plotted against $(h\nu)$, where α is the absorption coefficient and $h\nu$ is the photon energy. The formula shows that the optical absorption coefficient changes with photon energy $h\nu$ [23].

$$(\alpha h\nu) = A(h\nu - E_g)^n \quad (3)$$

Here A is a constant, E_g is the optical band gap and n is assumed to be $\frac{1}{2}$, respectively. Figure 4 shows the UV-Vis optical absorption spectra of MnS thin films. While the band gap of the unannealed MnS thin film is 3.31eV, the band gap of the MnS thin film annealed at 150°C decreases to 3.24eV. When the annealing temperature is 200°C, the band gap decreases to 3.17, at 250°C to 3.14, and at 300°C

to 3.11 eV. It is sighted that the band gap of MnS semiconductor thin films decreases with the effect of annealing temperature. Reddy et al., and Girish et al. investigated the optical properties of MnS thin films depending on the annealing temperature using different physicochemical methods and, found that the band gap decreases with the increase in annealed temperature [16, 26]. As the annealing temperature increases, the crystallinity of MnS thin films improves, leading to larger grain sizes. The reduction in grain boundaries minimizes quantum confinement effects, which are more pronounced in smaller grains. Larger grains result in a decrease in the band gap due to reduced electron confinement. This trend is consistent with the XRD results, where higher annealing temperatures show increased grain size and improved crystal structure. Annealing reduces structural defects such as dislocations, vacancies, and interstitials. These defects can introduce localized states in the band gap. As these defects are minimized, the effective band gap narrows because the density of localized states decreases, and the conduction and valence bands become more well-defined. At higher annealing temperatures, the MnS thin film may undergo changes in stoichiometry or phase composition. For instance, annealing might promote the formation of specific MnS phases with narrower band gaps. Any secondary phases or improved stoichiometric uniformity could influence the electronic structure, leading to a decrease in the band gap.

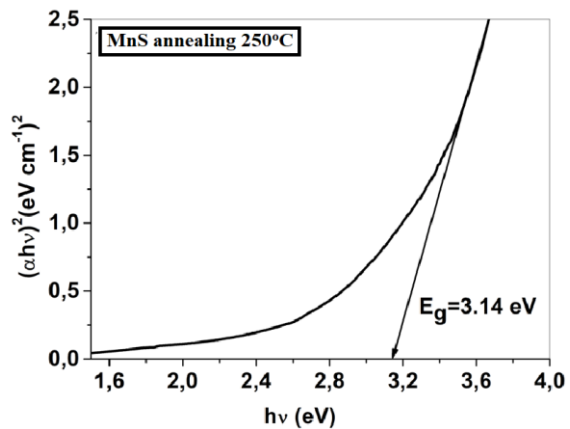
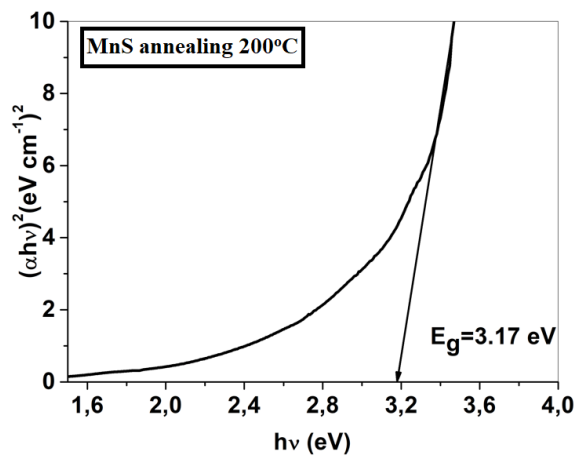
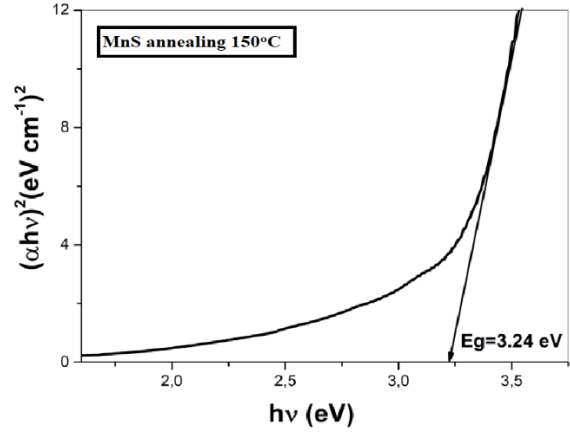
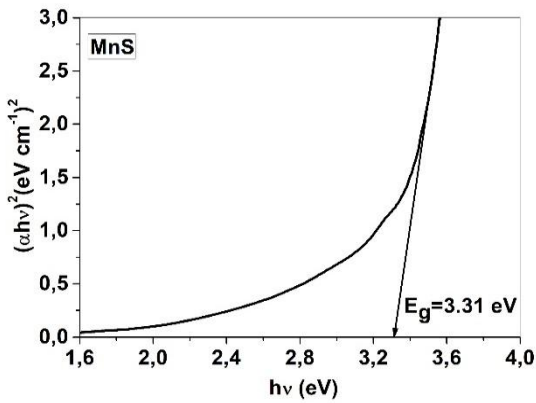


Figure 4. (Cont.) UV-vis spectra of unannealed, 150°C, 200°C, 250°C, and 300°C annealed MnS thin films.

Figure 4. UV-vis spectra of unannealed, 150°C, 200°C, 250°C, and 300°C annealed MnS thin films.

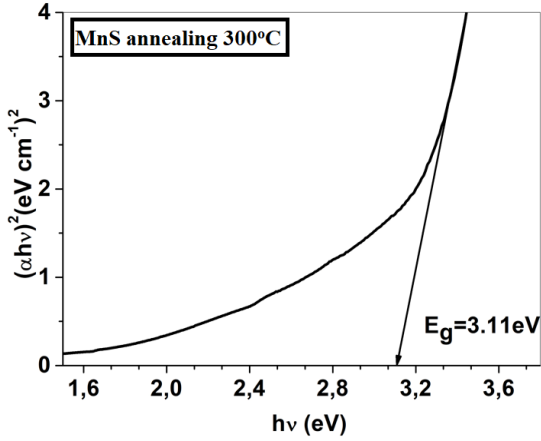


Figure 4. (Cont.) UV-vis spectra of unannealed, 150°C, 20°C, 250°C, and 300°C annealed MnS thin films.

MnS thin film was grown to a thickness by Çayır Taşdemirci using the SILAR method. When MnS thin films were grown depending on the annealing temperature, significant differences emerged in the results. XRD peak intensities increased and depending on this situation, grain size value increased from 9.20 nm to 13.36 nm when grown depending on thickness, while it increased from 11.66 nm to 43.6 nm when examined depending on annealing temperature. FWHM value decreased from 0.9 to 0.62 when depending on thickness, and FWHM value decreased from 0.71 to 0.19 with the effect of an annealing temperature. The dislocation density value also decreased from $118 \times 10^{-4} \text{cm}^{-2}$ to $56 \times 10^{-4} \text{cm}^{-2}$. when it was dependent on the thickness, while it decreased from $73 \times 10^{-4} \text{cm}^{-2}$ to $5 \times 10^{-4} \text{cm}^{-2}$ with the effect of annealing temperature. When the energy band gap value was examined as a function of the thickness, it decreased from 3.32 eV to 3.02 eV, and when it was examined as a function of the annealing temperature, it decreased from 3.31 eV to 3.11 eV. When the effects of the thickness and annealing temperature, which are among the parameters of the SILAR method, on the MnS thin films were examined, we can say that the effect of the annealing temperature on the physical properties of the MnS thin films was better.

4. Conclusions

The annealing temperature is one of the important parameters for the SILAR method, which is among the thin film growth techniques. The effect of annealing temperature on thin films is also included in many studies in literature. The effect of annealing temperature on MnS thin films was investigated. UV-Vis and XRD results confirmed that the SILAR method is effective for MnS film growth. MnS thin films were subjected to different annealing temperatures.

XRD results revealed that the annealing temperature increased the peak intensity. At the same time, it was observed that the grain size increased from 11.66 nm to 43.6 nm and the dislocation density decreased from $73 \times 10^{-4} \text{cm}^{-2}$ to $5 \times 10^{-4} \text{cm}^{-2}$. SEM results supported XRD results, and the effect of surface annealing temperature became more homogeneous. Optical measurements revealed that the band gap energy of MnS thin films decreased from 3.31 eV to 3.11 eV with the annealing temperature. The band gap of 3.11–3.31 eV falls within the ultraviolet (UV) and visible light range, making MnS thin films useful in UV photodetectors, light-emitting diodes (LEDs), and laser diodes.

Declaration of Ethical Standards

If the study does not require an Ethics Approval, the following declaration can be used:

“There are no ethical issues regarding the publication of this study.”

Conflict of Interest

The author declares that there are no personal relations or financial interests that could negatively affect this work.

References

- [1] Pujari R.B., Lokhande A.C., Yadav A.A., Kim J.H., Lokhande C.D., 2016. Synthesis of MnS microfibers for high-performance flexible supercapacitors. *Materials & Design*, **108**, pp.510-517.
- [2] Wang S., Li K., Zhai R., Wang H., Hou Y., Yan H., 2005. Synthesis of metastable γ -manganese sulfide crystallites by microwave irradiation. *Materials Chemistry and Physics*, **91**, pp.298-300.
- [3] Zhao P., Zeng Q., He X., Tang H., Huang K., 2008. Preparation of γ -MnS hollow spheres consisting of cones by a hydrothermal method. *Journal of Crystal Growth*, **310**, pp. 4268-4272.
- [4] Hernández S.A.M., Sandoval S.J., Pérez R.C., Delgado G.T., Chao B.S., Sandoval O.J., 2003. Preparation and characterization of polycrystalline MnS thin films by the RF-sputtering technique above room temperature. *Journal of Crystal Growth*, **256**, pp.12-19.
- [5] Gümüş C., Ulutaş C., Ufuktepe Y., 2007. Optical and structural properties of manganese sulfide thin films. *Optical Materials*, **29**, pp.1183-1187.

- [6] Ulutaş C., Gumus C., 2016. Annealing effect on structural and optical properties of chemical bath deposited MnS thin film. AIP Conference Proceedings, 2016, **1722**, pp.080008
- [7] Gümüş C., Ulutaş C., Esen O. M., Özkendir R., Ufuktepe Y., 2005. Preparation and characterization of crystalline MnS thin films by chemical bath deposition. Thin Solid Films, **492**, pp 1-5.
- [8] Hannachi A., Maghraoui-Meherzi H., 2017. Growth of different phases and morphological features of MnS thin films by chemical bath deposition: Effect of deposition parameters and annealing. Journal of Solid State Chemistry, **247**, pp. 120-130.
- [9] Hannachi A., Hammami S., Raouafi N., Maghraoui-Meherzi H., 2016. Preparation of manganese sulfide (MnS) thin films by chemical bath deposition: Application of the experimental design methodology. Journal of Alloys and Compounds, **663**, pp. 507-515.
- [10] Pahtan H.M., Kale S.S., Lokhande C.D., Han S.H., Joo O.S., 2007. Preparation and characterization of amorphous manganese sulfide thin films by SILAR method. Materials Research Bulletin, **42**, pp. 1565-1569.
- [11] Moreno-García H., Sigala-Valdez J.O., Martínez Blanco Ma del R., Cruz Reyes I., Durón-Torres S.M., Escalante-García I.L., Del Rio-De Santiago A., 2024. Effect in variation of the cationic precursor temperature on the electrical and crystalline properties of MnS growth by SILAR. Heliyon, **10**, pp. e26703.
- [12] Liu X., Zhang Y., Zhang Y., Bi Z., Zhou J., Xu R., Ruan S., 2025. High response MSM UV photodetectors based on MgZnO/MnS heterojunction. Materials Science in Semiconductor Processing, **185**, pp.108946-108953.
- [13] Zheng Z., Liu D., Sun X., Geng Z., Wang Q., Hou J., 2025. SILAR synthesis of CdS-ZnS/TiO₂ NTs for photocatalytic H₂ evolution and dye degradation. Colloids and Surfaces A: Physicochemical and Engineering Aspects, **707**, pp.135922-135932.
- [14] Lee W.J., Hsua T. W., Lee W.L., Thaia T. T., Chen C. C., 2025. Surface modification of carbon felt electrodes with SnO₂ nanocoatings by using the SILAR method for enhanced performance in vanadium redox flow batteries. Applied Surface Science, **686**, pp.162150-162162.
- [15] Tan H. J., Shafie S., Zainal Z., Tan S. T., Talib Z. A., Bahrudin N. N., 2025. ZnO nanorods anchored SnS through successive ionic layer adsorption and reaction (SILAR) approach for enhanced performance photoelectrochemical cell. Applied Materials Today, **42**, pp.102581-102591.
- [16] Reddy D.S., Reddy D.R., Reddy B.K., Reddy A.M., Gunasekhar K.R., Reddy P.S., 2007. Annealing effect on physical properties of thermally evaporated MnS nanocrystalline films. Journal Optoelectronic Advanced Materials, **9**, pp.2019-2022.
- [17] Hannachi A., Segura A., Maghraoui-Meherzi H., 2016. Growth of manganese sulfide (a-MnS) thin films by thermal vacuum evaporation: Structural, morphological and optical properties. Materials Chemistry and Physics, **181**, pp. 326-332.
- [18] Tigwera Gervais A., Khan Malik D., Nyamen Linda D., Aboud Ahmed A., Moyo T., Dlamini Sanele T., Ndifon Peter T., Revaprasadu N., 2022. Molecular precursor route for the phase selective synthesis of α -MnS or metastable γ -MnS nanomaterials for magnetic studies and deposition of thin films by AACVD. Materials Science in Semiconductor Processing, **139**, pp.106330-106339.
- [19] Yıldırım M. A., Yıldırım S. T., Cavanmirza İ., Ateş A., 2016. Chemically synthesis and characterization of MnS thin films by SILAR method. Chemical Physics Letters, **647**, pp. 73-78.
- [20] Chaki S. H., Chauhan S. M., Tailor J. T., Deshpande M. P., 2017. Synthesis of manganese sulfide (MnS) thin films by chemical bath deposition and their characterization. Journal of Materials Research and Technology, **6**, pp. 123-128.
- [21] Yang Q., Chen Q., Gong F., Li Y., 2023. Fabrication of MnCoS Thin Films Deposited by the SILAR Method with the Assistance of Surfactants and Supercapacitor Properties. Coating, **13** pp. 908-920.
- [22] Tiwari P., Jaiswal J., Chandra R., 2019. Optical and electrical properties of highly ordered α -, γ - and $\alpha + \gamma$ -MnS films deposited by reactive sputtering technique. Journal of Applied Physics, **126**, 213108-213120.
- [23] Taşdemirci T.Ç., 2020. Copper Oxide Thin Films Synthesized by SILAR: Role of Varying Annealing Temperature. Electronic Materials Letters, **16**, pp.239-246.
- [24] Akaltun Y., 2023. Fabrication and Characterization of NiSe₂ Films Prepared by SILAR Method. IEEJ Transactions on Electrical and Electronic Engineering, **18**, pp.1414-1418.
- [25] Biswas S., Kar S., Chaudhuri S., 2007. Effect of the precursors and solvents on the size, shape and crystal structure of manganese sulfide crystals in solvothermal synthesis. Materials Science Engineering B, **142**, pp.69-77.

[26] Girish M., Dhandayuthapani T., Sivakumar R., Sanjeeviraja C., 2015. MnS thin films prepared by a simple and novel nebulizer technique: report on the structural, optical, and dispersion energy parameters. *Journal of Materials Science: Materials Electron*, **26**, pp.3670-3684.

[27] Çayır Taşdemirci T., 2025. Synthesis of MnS thin film: investigation of thickness-dependent physical properties. *Indian Journal of Physics*, pp. 1-8.